

Collaborative research from the University of Cincinnati (USA) and the University of Bordeaux (France).

Mechanically tunable PDMS-based polyHIPE acoustic materials

Porous PDMS materials were prepared with emulsion templating. Acoustic analysis showed that these materials were able to reduce longitudinal sound speed through the materials to ~40 m/s.

As featured in:



See Neil Ayres *et al.*,
J. Mater. Chem. C, 2022, **10**, 6222.

COMMUNICATION



Cite this: *J. Mater. Chem. C*, 2022,
10, 6222

Received 10th January 2022,
Accepted 21st March 2022

DOI: 10.1039/d2tc00136e

rsc.li/materials-c

Polymer-based acoustic metamaterials possess properties including acoustic wave manipulation, cloaking, and sound dampening. Here, PDMS-based elastomers were prepared using thiol-ene “click reactions” with emulsion templating. Acoustic analysis showed these materials achieved sound speed values of $\sim 40 \text{ m s}^{-1}$, close to the predicted minimum of $\sim 25 \text{ m s}^{-1}$ attainable.

Introduction

Metamaterials are man-made materials that possess properties not found in nature, for example a negative refractive index^{1,2} or characteristics allowing for the realization of a lens with a sub-wavelength diffraction limit.³ Metamaterials have been proposed for use in applications which often rely on highly specific manufacturing of metals^{1,4} or composites⁵⁻⁷ in perfectly ordered structures such as high resolution lenses,^{3,8} wireless power transfer,⁹ and cloaking devices.¹⁰ While these technologies possess exciting possibilities, the manufacture of some metamaterials can be costly due to, for example, the advanced fabrication protocols required. A class of metamaterials described as soft *mechanical* metamaterials, can be prepared by simple additive manufacturing (or 3D printing) techniques of elastomeric polymer networks to obtain negative or zero Poisson’s ratios.¹¹⁻¹⁴ Soft mechanical metamaterials have been prepared from commercially available polymers including poly(lactic acid),¹² poly(amide),¹¹ and polysiloxanes^{15,16} Furthermore, polysiloxanes have also been used¹⁷ or considered¹⁸ for the preparation of soft acoustic metamaterial waveguides having controlled acoustic wave manipulation. Specifically, for porous polysiloxane acoustic

metamaterials,¹⁹⁻²³ a strong dependence of the longitudinal sound speed on the porosity and material properties has been established. For example, it was reported¹⁹ that the stiffness of a polymer matrix around air-filled voids had a significant impact on the acoustic dampening performance of porous elastomers. It was demonstrated that the introduction of air cavities in stiff poly(styrene-*co*-divinylbenzene) materials did not change the speed of an acoustic wave travelling through the material, while PDMS networks prepared through a hydrosilylation reaction reduced the longitudinal sound speed (C_L) to around 50 m s^{-1} at a porosity of 36% in the material. That work highlighted the importance for obtaining a wide range of network stiffnesses to prepare targeted acoustic metamaterials that have predictable and controllable sound dampening capabilities. A simple and robust method to prepare both stiff and soft porous polymer networks is using an emulsion templating technique known as polymerized high internal phase emulsions (polyHIPEs).²⁴⁻²⁷ While soft acoustic polyHIPE-based metadevices have been reported, these examples have been limited to commercially available curable PDMSs, where only the volume fraction of the pores in the final polyHIPEs can be controlled to prepare the targeted wave shaping capabilities. In the work reported here, we proposed targeting manipulating the network chemistry of PDMS-based polyHIPE elastomers to control the storage modulus of the materials. To achieve this, we used thiol-ene “click reactions” as a simple and robust polymerization technique to control the crosslinking in the network which in turn controlled the moduli of materials, with the goal of ultimately accessing a wider scope of desirable sound speeds. Thiol-ene reactions²⁸⁻³⁰ have been widely reported in controlling crosslinking density of polymeric networks to dictate mechanical properties in applications such as biomaterials,³¹ covalent adaptable networks³² and soft electronics.³³ Thiol-ene reactions have also been shown to be compatible with polyHIPE syntheses containing small molecule components^{34,35} and macromolecules.³⁶ For example, in previous studies from our lab we prepared polyHIPEs using thiol- and vinyl-functionalized PDMSs.³⁶

^a Department of Chemistry, The University of Cincinnati, P.O. Box 210172, Cincinnati, Ohio 45221, USA. E-mail: neil.ayres@uc.edu

^b University of Bordeaux – CNRS, Centre de Recherche Paul Pascal, Pessac, France

^c University of Bordeaux – CNRS – Bordeaux INP, Institut de Mécanique et d’Ingénierie, Talence, France

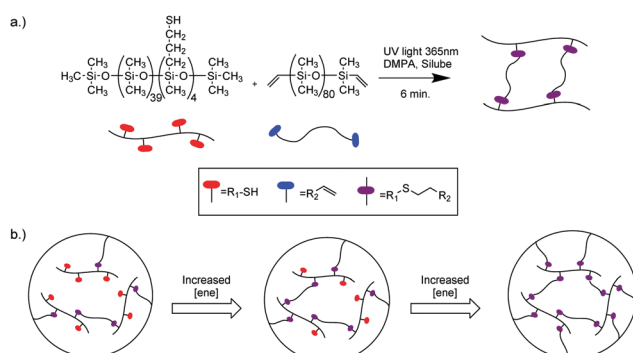
† Electronic supplementary information (ESI) available: Synthesis protocols and properties of non-porous controls. See DOI: 10.1039/d2tc00136e

Results and discussion

In this work, we prepared PDMS elastomers using thiol-ene click reactions (Scheme 1a) following our reported protocols,^{36,37} where the ratio of thiol-functionalized PDMS and vinyl-terminated PDMS was systematically changed to control crosslinking density (Scheme 1b).

We prepared both porous and non-porous materials in this work, where the non-porous PDMS materials are used as controls during acoustic measurements to establish the maximum sound speed of ultrasonic waves traveling through a non-porous matrix. We have named our materials on the basis of the thiol to ene molar ratio used in their synthesis and if the material is a polyHIPE or the non-porous control material. For example, we name a polyHIPE prepared using a thiol to ene ratio of 3:1 as PH_{3:1} whereas the non-porous PDMS film prepared using a thiol to ene ratio of 3:1 is denoted as NP_{3:1}. We varied the functional group molar ratio from a 1:1 thiol/ene ratio to various degrees of excess thiol or alkene content to explore a wide range of possible network chemistries. We selected a constant targeted total porosity value (Φ_{theo}) of 40% and a constant concentration of the surfactant, Silube, of 1.0 wt % with respect to total PDMS in the polyHIPEs to isolate the effects of the thiol-ene ratio on the mechanical strength of polyHIPEs. We chose these conditions based on our previous work³⁶ preparing polyHIPEs for acoustic metamaterials where a polyHIPE with a targeted total porosity of 40% was seen to reduce C_L to approximately 40 m s⁻¹. While conventionally a Φ_{theo} of 40% is formally called a polyMIPE, as it is a *medium* internal phase emulsion, we have used the more common polyHIPEs descriptor for consistency in naming across other related work. Porous and non-porous materials were characterized using scanning electron microscopy (SEM), density measurements, total porosity calculations, dynamic mechanical analysis (DMA), and ultrasonic acoustic analysis.

The calculated experimental total porosity, Φ_{exp} , of the polyHIPEs was calculated using eqn (1) where ρ_0 is the average density of the bulk PDMS (0.975 g mL⁻¹), ρ^* is the measured



Scheme 1 Crosslinking reaction between thiolated-PDMS and vinyl-PDMS for (a) the general thiol-ene polymerization and (b) how crosslinking density is controlled by increasing the concentration of vinyl-PDMS. A commercially available surfactant, Silube, was used to stabilize the emulsions. 2,2-Dimethoxy-2-phenylacetophenone (DMPA) was used as the photoinitiator for both polyHIPEs and non-porous films.

Table 1 Measured density and total porosity of PDMS polyHIPEs (PH_{3:1}–PH_{1:3})

polyHIPE	Measured density (g mL ⁻¹)	Total porosity ^a (±2%)
PH _{3:1}	0.625	38
PH _{2:5:1}	0.610	39
PH _{2:1}	0.607	38
PH _{1.5:1}	0.622	36
PH _{1:1}	0.617	38
PH _{1:1.5}	0.651	42
PH _{1:2}	0.601	40
PH _{1:2.5}	0.599	37
PH _{1:3}	0.625	41

^a Calculated from eqn (1).

density of individual polyHIPE samples, and the results are shown in Table 1.

$$1 - \frac{\rho^*}{\rho_0} = \Phi_{\text{exp}} \quad (1)$$

Changing the thiol to ene ratio in the polyHIPE series did not affect the calculated total porosity and the measured densities, where all samples possessed similar measured densities resulting in polyHIPEs with a total porosity of around 40%. We anticipated little or no change in Φ_{exp} when changing only the cross-linking chemistry within the network, as the polyHIPE method is a templating process dependent on the volume of dispersed phase. We observed a density value closely related to bulk PDMS for the non-porous samples resulting in a calculated Φ_{exp} of zero (Table S1, ESI†).

Porous polyHIPEs and non-porous materials were characterized using SEM to obtain qualitative estimates about pore size and pore morphology (Fig. 1).

Fig. 1a shows the SEM image of polyHIPE PH_{1:1} possessing a partially interconnected porous structure with a dispersity in pore sizes. The dispersity in observed pore sizes and the spherical nature of the pore structure are direct results of the templating process caused by the aqueous water droplets formed during emulsification. We also observe sections of the

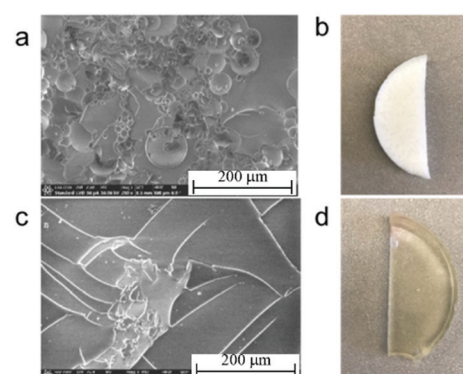


Fig. 1 Cross sectional SEM (a and c) and digital (b and d) images of polyHIPE PH_{1:1} (a and b) and non-porous film NP_{1:1} (c and d). Scale bar is 200 μ m for the SEM images. PDMS samples were prepared in a 35 mm \times 3 mm ($w \times h$) circular mold.

material where the surface is smooth consisting of regions of non-porous bulk PDMS. This partially interconnected pore structure has been previously observed^{23,36,37} as the aqueous dispersed phase droplets prefer an aggregated morphology when Silube is used as the surfactant in water-in-PDMS emulsions.

The non-porous material, NP_{1:1}, possesses a smooth surface with slight ripples due to cutting the film with a razor blade confirming that the material is non-porous as was expected (Fig. 1c). Digital images of these materials in Fig. 1b and d show the clear difference in optical properties between porous and non-porous samples, where the presence of pores results in an opaque white foam (Fig. 1b) compared to a transparent film in the NP_{1:1} material (Fig. 1d). These SEM and digital images are representative of all the formulations where no differences were observed when changing the thiol to ene ratio. These SEM results were similar to those in our previous work,³⁶ which showed the most significant impact on pore size and morphology were due the volume fraction of the dispersed phase in the emulsion formulation and the concentration of surfactant used to stabilize the HIPE. We kept these two parameters constant in this study.

The viscoelastic properties of the materials were characterized using frequency sweep experiments to obtain the storage moduli (G') (Fig. 2). The storage moduli observed in polyHIPEs with changing stoichiometric molar ratio of thiol to 'ene' functional groups are plotted in Fig. 2a. Two trends can be observed in this data. First, G' increases as the concentration of vinyl-terminated PDMS is increased until a 1:1 stoichiometric ratio is reached. For example, PH_{3:1} had the highest excess thiol content and a storage modulus of ~ 75 kPa, while PH_{1:1} with no excess thiol content possessed a storage modulus of ~ 225 kPa. We see an increase of around 30 kPa in the storage modulus for every 0.5 mole ratio increase of 'ene' content with respect to the thiol content. The same trend is observed when excess double bonds are introduced into the polymer network, but with a different magnitude in the response. For example, when a small excess of the vinyl-terminated PDMS was present in the formulation for polyHIPE PH_{1:1.5}, a decrease of ~ 130 kPa was observed from PH_{1:1}. This trend continued in polyHIPE PH_{1:2} and increasing the ratio of vinyl groups to thiols in polyHIPEs PH_{1:2.5} and PH_{1:3} resulted in materials that were too tacky and

weak to be characterized using DMA. We observed the same trend in storage moduli with stoichiometric ratio of thiol:ene in the non-porous films as we did for the polyHIPEs, albeit at a higher magnitude (Fig. 2b). A balanced thiol to ene ratio in NP_{1:1} resulted in the highest G' of ~ 1150 kPa and excess vinyl-functional groups reduced the storage moduli of NP_{1:1.5}, NP_{1:1.2}, and NP_{1:2.5}. This effect again caused the formulation with the highest content of excess vinyl groups, NP_{1:3}, to be too weak to be characterized using DMA. These results for our polyHIPEs and non-porous PDMS elastomers show that a balanced thiol to ene ratio produced materials with the strongest networks regardless of the presence of pores in the network. An increase in storage moduli was observed when varying the thiol to ene ratios from 3:1 to 1:1 due to increasing crosslinking density with the increasing vinyl-terminated PDMS. Further addition of vinyl-terminated PDMS in formulations (thiol to ene ratios from 1:1.5 to 1:3) significantly decreased the network strength presumably due to unreacted vinyl-groups acting as network defects in the form of dangling chain ends.³⁸ Interestingly, these results from mechanical analysis of our materials differ from other findings in the literature with crosslinked PDMS elastomers prepared using thiol-ene click reactions, where it was reported that an excess thiol content was needed to overcome potential network defects and weak elastomers.³⁹ In that work, Gautrot and co-workers³⁹ prepared PDMS films using a high thiol content poly([mercaptopropyl]methyl siloxane) homopolymer and various lengths of vinyl terminated PDMS crosslinkers. A molar ratio of 2:1 (thiol:ene) thiolated- and vinyl-PDMS produced the strongest networks independent of the crosslinker, which the authors attributed to incomplete consumption of the alkene at equal stoichiometric ratios due to primary network defects. Our system appears to more closely resemble the results of thiol-ene crosslinked PDMS from Müller and Kunze⁴⁰ using a lower thiol-content PDMS copolymer and an equal thiol to ene ratio produced PDMS elastomers with the highest crosslink density. Taken together, these results suggest that the relative density of thiol functional groups on the PDMS chain may play a role in how network defects affect the final materials.

The acoustic properties of non-porous and polyHIPE materials were characterized at ultrasonic frequencies to test their potential use as acoustic metamaterials. For non-porous PDMS samples NP_{3:1}–NP_{1:3}, the longitudinal sound speeds inside these samples were similar and ~ 1000 m s⁻¹ (Table S1, ESI[†]) similar to results in previous studies of non-porous PDMS materials.^{19–22} The acoustic analysis was performed on porous polyHIPE materials PH_{3:1}–PH_{1:3} and the values are given in Fig. 3. Unfortunately, measurements could not be performed on all the polyHIPEs, as those with the lowest moduli (*i.e.*, PH_{3:1}, PH_{2.5:1}, PH_{1:2.5}, and PH_{1:3}) were too delicate to be manipulated between the transducers. In these measurements, the C_L measured for non-porous PDMS, ~ 1000 m s⁻¹, acts as an upper boundary condition to isolate the impact of matrix stiffness, *i.e.*, thiol to ene ratio, on C_L when a defined volume of air-filled pores have been introduced to the matrix.

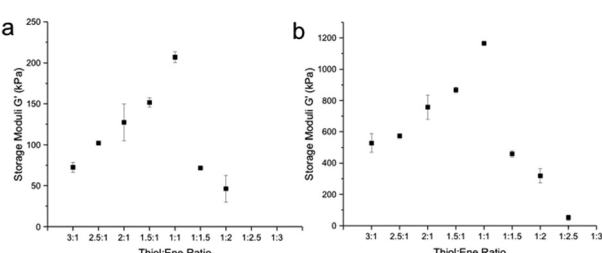


Fig. 2 Storage modulus versus thiol to ene ratio of (a) polyHIPEs PH_{3:1}–PH_{1:3} and (b) non-porous films NP_{3:1}–NP_{1:3}. During frequency sweeps, no variation in the storage moduli was observed over the frequency range used so an average of three replicates at 10 Hz is used.

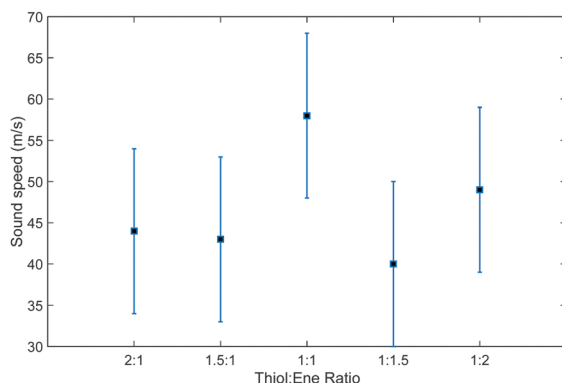


Fig. 3 Sound speed versus thiol to ene ratio of polyHIPEs PH_{2:1}–PH_{1:2}.

As can be seen in Fig. 3, for the polyHIPEs that were suitable for ultrasonic testing, low values of the longitudinal sound speed of $\sim 40 \text{ m s}^{-1}$ were obtained. These polyHIPE materials show slower longitudinal sound speeds than comparable gas-filled siloxane aerogels^{41,42} and gas-filled balloon doped polyurethanes.⁴³ Specifically, Gross and Fricke⁴¹ observed sound speeds of $\sim 100 \text{ m s}^{-1}$ while Du and co-workers⁴² found aerogels made from siloxanes having pendent backbone functionality resulted in sound speeds of $\sim 150 \text{ m s}^{-1}$.

Interestingly, in the materials presented in our work, the sound speed appears to be very weakly dependent on the storage moduli but exhibits a maximum for the thiol:ene ratio of 1:1, *i.e.*, when the storage modulus of the non-porous matrix is the highest as shown in Fig. 2b. Such dependence has been already observed in soft porous materials by Kovalenko *et al.*¹⁹ and is well-captured by the Kuster–Toksöz model. These results agree with our previous work where a PDMS polyHIPE with similar porosities obtained sounds speeds of $\sim 40 \text{ m s}^{-1}$.³⁶ In that previous work, only a single polyHIPE was tested for its acoustic performance. The results from our current work therefore represent a more comprehensive study in how the cross-linking density in polyHIPEs affect their materials properties and thus their ultimate acoustic performances.

It is worth noting that for very soft porous materials, when the storage modulus becomes much smaller than the air bulk modulus ($\approx 130 \text{ kPa}$) the equation linking the sound speed to the porosity will reduce to:

$$C_L = \sqrt{\frac{K_{\text{air}}}{\rho_0 \Phi(1 - \Phi)}} \quad (2)$$

This expression is similar to the Wood mixing law traditionally used for bubbly liquids⁴⁴ but that also applies for very soft porous materials. In this case, the longitudinal sound speed (C_L) no longer depends on the storage modulus of the material, as observed in our polyHIPE samples. Considering the porosity of our samples is approximately 40%, we can calculate that $C_L \approx 25 \text{ m s}^{-1}$ using Eqn 2, which can be thought of as the lowest possible attainable sound speed in soft porous polymer systems. The polyHIPEs reported here with remarkably low values of longitudinal sound speeds could be appropriate for

use in acoustic metadevices.^{22,23} Our future work will focus on preparing PDMS-based polyHIPEs with wider ranges of storage moduli and at multiple porosities for the realization of acoustic metadevices that can precisely control the sound speed of travelling acoustic waves.

Conclusions

The work presented here demonstrates our ability to prepare porous and non-porous PDMS elastomers possessing mechanical properties that are predictable and dependent on the thiol to ene ratio of the polymer network. Both porous and non-porous materials showed identical trends in mechanical properties where an equal thiol to ene molar ratio produced materials with the highest storage modulus of ~ 225 and $\sim 1150 \text{ kPa}$ respectively. As expected, non-porous PDMS elastomers were found to all obtain similar longitudinal sound speeds of $\sim 1000 \text{ m s}^{-1}$ during ultrasonic characterization. Acoustic measurements of polyHIPEs show that all materials obtain exceptionally low values of sound speed of about 40 m s^{-1} , regardless of the thiol to ene ratio. These results show that these polyHIPE formulations have promise as acoustic metamaterials.

Author contributions

T. J. M.: investigation, methodology, visualization, writing; K. R.: investigation; S. S.: investigation; O. M. M.: conceptualization, methodology, formal analysis, writing, resources; T. B.: conceptualization, methodology, formal analysis, writing, resources; N. A.: conceptualization, project management, resources, supervision, writing.

Conflicts of interest

There are no conflicts to declare.

Acknowledgements

T. J. M., K. R., S. S., and N. A. thank the National Science Foundation (DMR-1940518) for the resources to conduct this work. N.A. thanks Mr. Spencer Hendrickson and Dr Ryan White for help preparing the 3D printed molds used in this work, and Dr Melodie Fickenscher for help with acquiring the SEM images. T. B. and O. M. M. thank the Labex AMADEUS ANR-10-LABEX-0042-AMADEUS with the help of the French state Initiative d'Excellence IdEx ANR-10-IDEX-003-02 the project BRENNUS ANR-15-CE08-0024 (ANR and FRAE funds) for the resources to conduct this work.

References

- 1 R. A. Shelby, D. R. Smith and S. Schultz, *Science*, 2001, **292**, 77.
- 2 D. R. Smith, J. B. Pendry and M. C. K. Wiltshire, *Science*, 2004, **305**, 788–792.

3 N. Fang, H. Lee, C. Sun and X. Zhang, *Science*, 2005, **308**, 534–537.

4 N. I. Landy, S. Sajuyigbe, J. J. Mock, D. R. Smith and W. J. Padilla, *Phys. Rev. Lett.*, 2008, **100**, 1–4.

5 G. V. Naik, V. M. Shalaev and A. Boltasseva, *Adv. Mater.*, 2013, **25**, 3264–3294.

6 P. Schürch and L. Philippe, *Encycl. Mater. Compos.*, 2021, **2**, 390–401.

7 D. R. Smith, W. J. Padilla, D. C. Vier, S. C. Nemat-Nasser and S. Schultz, *Phys. Rev. Lett.*, 2000, **84**, 4184–4187.

8 V. M. Shalaev, *Nat. Photonics*, 2007, **1**, 41–48.

9 C. Rong, C. Lu, Y. Zeng, X. Tao, X. Liu, R. Liu, X. He and M. Liu, *IET Power Electron.*, 2021, **14**, 1541–1559.

10 J. B. Pendry, D. Schurig and D. R. Smith, *Science*, 2006, **312**, 1780–1782.

11 H. Yang and L. Ma, *Mater. Des.*, 2020, **188**, 108430.

12 M. Bodaghi, A. R. Damanpack, G. F. Hu and W. H. Liao, *Mater. Des.*, 2017, **131**, 81–91.

13 C. Ren, D. Yang and H. Qin, *Materials*, 2018, **11**, 1078.

14 R. Hedayati, A. Güven and S. Van Der Zwaag, *Appl. Phys. Lett.*, 2021, **118**, 141904.

15 Y. Tang, G. Lin, L. Han, S. Qiu, S. Yang and J. Yin, *Adv. Mater.*, 2015, **27**, 7181–7190.

16 D. Goswami, S. Liu, A. Pal, L. G. Silva and R. V. Martinez, *Adv. Funct. Mater.*, 2019, **29**, 1–11.

17 R. M. Guillermic, M. Lanoy, A. Strybulevych and J. H. Page, *Ultrasonics*, 2019, **94**, 152–157.

18 J. Li and C. T. Chan, *Phys. Rev. E: Stat., Nonlinear, Soft Matter Phys.*, 2004, **70**, 055602.

19 A. Kovalenko, M. Fauquignon, T. Brunet and O. Mondain-Monval, *Soft Matter*, 2017, **13**, 4526–4532.

20 R. Kumar, Y. Jin, S. Marre, O. Poncelet, T. Brunet, J. Leng and O. Mondain-Monval, *J. Porous Mater.*, 2020, **28**, 249–259.

21 Y. Jin, R. Kumar, O. Poncelet, O. Mondain-Monval and T. Brunet, *Nat. Commun.*, 2019, **10**, 143.

22 K. Zimny, A. Merlin, A. Ba, C. Aristégui, T. Brunet and O. Mondain-Monval, *Langmuir*, 2015, **31**, 3215–3221.

23 A. Kovalenko, K. Zimny, B. Mascaro, T. Brunet and O. Mondain-Monval, *Soft Matter*, 2016, **12**, 5154–5163.

24 C. Stubenrauch, A. Menner, A. Bismarck and W. Drenckhan, *Angew. Chem., Int. Ed.*, 2018, **57**, 10024–10032.

25 M. S. Silverstein, *Prog. Polym. Sci.*, 2014, **38**, 199–234.

26 T. Zhang, R. A. Sangaramath, S. Israel and M. S. Silverstein, *Macromolecules*, 2019, **52**, 5445–5479.

27 N. R. Cameron, *Polymer*, 2005, **46**, 1439–1449.

28 Q. Li, H. Zhou and C. E. Hoyle, *Polymer*, 2009, **50**, 2237–2245.

29 M. J. Kade, D. J. Burke and C. J. Hawker, *J. Polym. Sci., Part A: Polym. Chem.*, 2010, **48**, 743–750.

30 C. E. Hoyle and C. N. Bowman, *Angew. Chem., Int. Ed.*, 2010, **49**, 1540–1573.

31 Y. C. Yeh, E. A. Corbin, S. R. Caliari, L. Ouyang, S. L. Vega, R. Truitt, L. Han, K. B. Margulies and J. A. Burdick, *Biomaterials*, 2017, **145**, 23–32.

32 K. Cheng, A. Chortos, J. A. Lewis and D. R. Clarke, *ACS Appl. Mater. Interfaces*, 2022, **14**, 4552–4561.

33 C. N. Walker, C. Versek, M. Touminen and G. N. Tew, *ACS Macro Lett.*, 2012, **1**, 737–741.

34 E. Lovelady, S. D. Kimmins, J. Wu and N. R. Cameron, *Polym. Chem.*, 2011, **3**, 559–562.

35 S. Caldwell, D. W. Johnson, M. P. Didsbury, B. A. Murray, J. J. Wu, S. A. Przyborski and N. R. Cameron, *Soft Matter*, 2012, **8**, 10344–10351.

36 T. J. McKenzie, P. S. Heaton, K. Rishi, R. Kumar, T. Brunet, G. Beaucage, O. Mondain-Monval and N. Ayres, *Macromolecules*, 2020, **53**, 3719–3727.

37 T. J. McKenzie, S. Smail, K. Rost, K. Rishi, G. Beaucage and N. Ayres, *Polymer*, 2021, **231**, 124116.

38 D. Chan, Y. Ding, R. H. Dauskardt and E. A. Appel, *ACS Appl. Mater. Interfaces*, 2017, **9**, 42217–42224.

39 K. D. Q. Nguyen, W. V. Megone, D. Kong and J. E. Gautrot, *Polym. Chem.*, 2016, **7**, 5281–5293.

40 U. Müller, A. Kunze, C. Herzig and J. Weis, *J. Macromol. Sci., Part A: Pure Appl. Chem.*, 1996, **33**, 439–457.

41 J. Gross and J. Fricke, *J. Non-Cryst. Solids*, 1992, **145**, 217–222.

42 Y. Xie, B. Zhou and A. Du, *Adv. Compos. Hybrid Mater.*, 2021, **4**, 248–256.

43 B. R. Matis, S. W. Liskey, N. T. Gangemi, Z. J. Waters, A. D. Edmunds, W. B. Wilson, D. M. Photiadis, B. H. Houston and J. W. Baldwin, *Langmuir*, 2020, **36**, 5787–5792.

44 A. B. Wood, *Textbook of Sound*, G. Bell & Sons, London, 1949.